

# Index of Refraction Lab Paper

Benjamin Schreyer

## 0.1 Abstract

The index of refraction and Snell's law are long standing concepts in physics, with Snell's law being linked to the very fundamental idea of least action. Our goal was to characterize two different materials in their property of index of refraction. To do this we first profiled a laser beam finding an intensity profile along a horizontal axes. We assured our laser had sufficiently ideal characteristics to use it in the two experiments which tracked the laser as it propagated through the two materials, a glass plate and acrylic block, in order to determine their indices of refraction.

## 0.2 Introduction

Covered in this paper will be methodology for laser characterization along on dimension, methodology for determining the index of refraction, and error analysis on an execution of these methods for determining the index of refraction.

The index of refraction is used in modeling many physical phenomena, such as reflection and deflection of light at boundary between media, which is clearly applicable to a wide range of phenomena.

## 0.3 Methods

**Beam Alignment** The laser diode was held in a two axis fine adjust mount, and featured a collimating lens. In all cases the collimating lens was adjusted to be as large as possible or as small as possible depending on the application (noted when described), this was done by eye by looking at the intersection of the laser with a target at the desired distance. To ensure the beam was held straight a variable distance and axes aligned target was used. By marking on the target where the beam center was located, then sliding the target along a guiding straight edge (deemed to be straight, and perpendicular, by mounting to pins on an optical breadboard) the beam could be inspected to ensure the intersection location on the target did not change within distinguish ability of the human eye. If the intersection location upon the two dimensional target varied with distance from laser diode to target, then the beam was deemed to not be pointing aligned along an axes of the optical breadboard, and the fine adjust mount was adjusted. This was repeated of order ten times until a human could not distinguish the beam intersection location as varying with distance between the target and the beam emitting diode.

**Beam Profiling** A programmable stepper motor horizontal stage was used to profile the beam. By mounting a photodiode with adjustable gain into the stage, or a blocking material (in our case a thick piece of paper when doing a blocking profiling) one could measure the laser's intensity along its beam, given that the stage and laser were perpendicular. The laser was aligned with our optical board as discussed above. The stage was aligned to the optical bread board by mounting it against pins into the board, ensuring a high level of perpendicularity.

To profile the beam using the photodiode alone, the photodiode was mounted into the translational stage, and its aperture closed until it produced signal when intersected by the laser, but was as small as possible. The aperture was chosen to be small to give the best possible lateral precision, as a larger aperture does not allow the beam to be probed as finely. Since the ratio of the beam width to the size of the aperture was to be maximized, the laser diode base lens was adjusted to yield the widest beam possible at the target (the horizontal stage). The diodes height was adjusted so that the beam height and photodiode height were the same. This gave the most fine grained spatial data that could be achieved with the limited time and material. A gain of 50dB was found to be ideal for the photodiode. To minimize signal to noise, your signal should be as large as possible, so the peak voltage read by the diode should near the 10V saturation point of the analog to digital conversion system. This was achieved in all cases with a gain of 50dB. By programmatically stepping the translation stage, and taking photodiode samples, the beam was profiled.

To profile the beam with a stationary photodiode and a moving blocking target, the beam was tuned to be as small as possible at the photodiode, so that it can fit onto the size of the photodiode chip, so that when the beam is fully unobstructed all emitted photons are incident on the sensor, and not the aperture or other sensor casing/mounting. The diodes height was adjusted so that the beam height and photodiode height were the same. The aperture was opened fully as the goal to collect data on the full range of the beam was to have as much of the beam incident on the sensor when unobstructed as possible. Then the blocking target was programmatically inserted or removed, taking photodiode samples as the blocking target's location varied by a single step. Errors involved are in alignment, moving stage inconsistencies, electrical noise (statistical), and vibration (statistical).

The beam characteristics were deemed workable which is described in detail in results.

**Index of Refraction for Plate Glass** Snell's Law uses the simple predictions of the principles of least action to predict the deflection of light rays incident upon media with changing indices of refraction. Data from an experimental setup to be described was fit to this model to determine the index of refraction

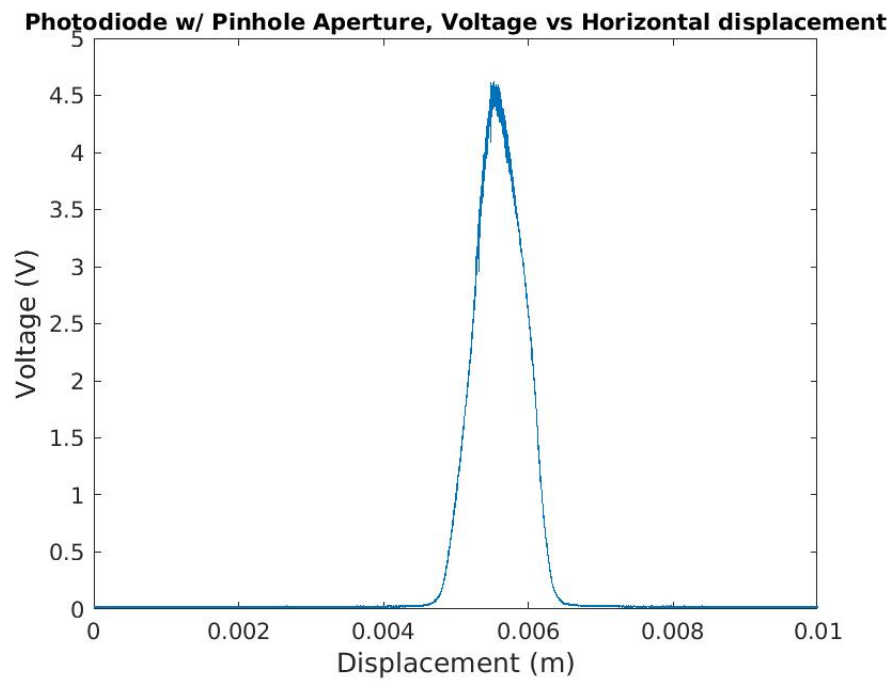
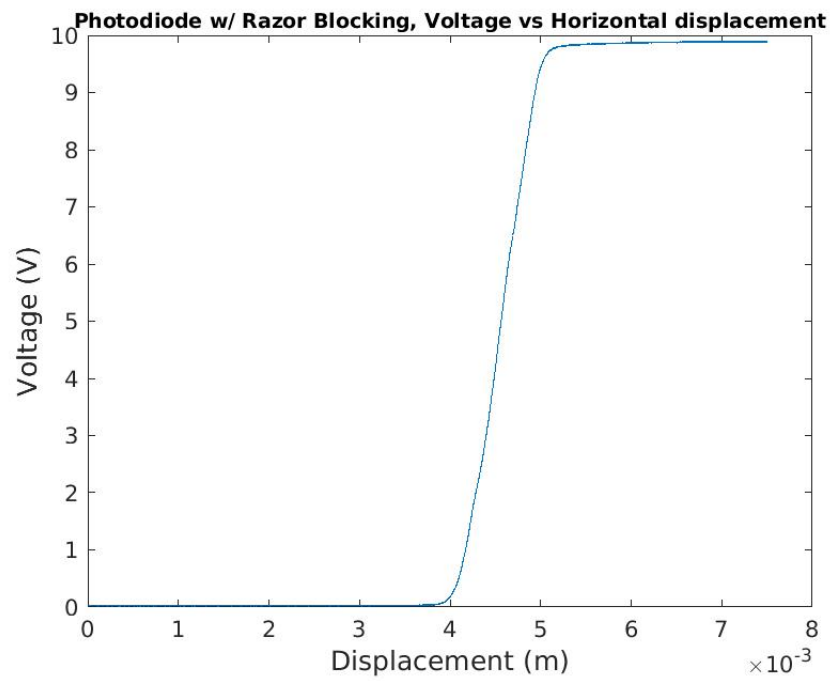
of a glass block. The laser was incident upon the glass block which was placed on a rotating stage with an incident angle  $\theta$ , the index of refraction of the plate,  $n$  two, and the index of refraction of air  $n$  one, the lateral displacement  $d$ , and the thickness of the glass plate  $L$  are related according to Snell's Law as follows.

$$\sin^2(\theta)(1 + \frac{\cos^2(\theta)}{(\sin(\theta) - \frac{d}{L})^2}) = (\frac{n_{glass}}{n_{air}})^2 \quad (1)$$

To determine the incident angle, the beam was aligned as described previously, and then a “jiggling” technique was used to align the rotational stage. According to Snell's Law an incident beam sees no deflection  $d$  when incident on a flat change of media (perpendicular to propagation). The beam was sent through the glass media on the rotational stage and then onto a paper target. The glass was then jiggled in and out of the path of the laser, while still being aligned to the stage. When beam position did not jiggle with the change of intersection with the glass media, then the beam was determined to be at zero degrees, and the moving stage's angle setting was read off to give a reference zero.

The beam was then adjusted to be as small as possible at the target of the photo diode, which was placed right after the moving stage with obstructing target. It was ensured that to the visible eye the entire beam fell upon the photodiode's silicon chip no matter what horizontal deflection was achieved via refraction. This is of great importance to making sure that the beam is profiled fully for all lateral displacements needed for the experiment.

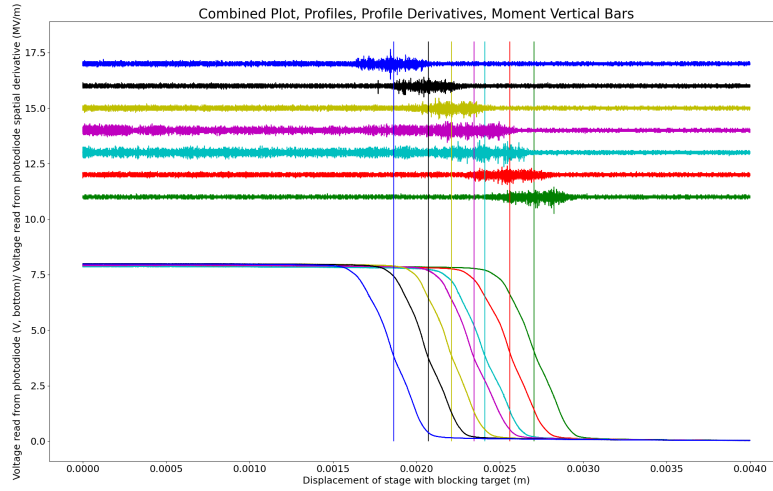
To take beam profile data for each angle of the glass media boundaries, the stage was swept across a 4mm range, to profile the beam fully by giving data points for the beam being fully obstructed, partially obstructed, and unobstructed. A single beam profile had the following form as data retrieved by the computer:



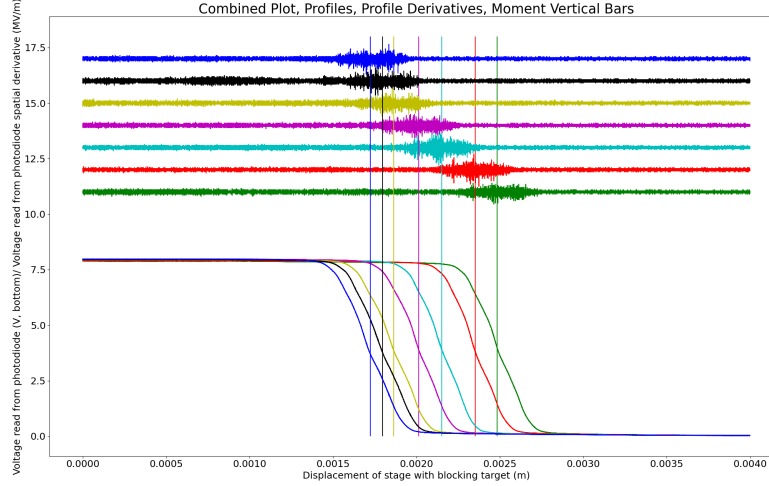
### 0.3 Methods

---

Fourteen such profiles were collected to characterize the material. The spatial derivatives of the profiles were taken, to return them to Gaussian form. All laser light is incident on the photodiode with no blocking, each decrease in blocking reveals an additional and small new portion of the beam to be incident upon the photodiode, giving an integral form of the beam profile. Then the derivative form's first order moment was determined to give a center for the beam. This yields a low uncertainty, as the moment is a weighted sum of many data points of which there are thousands. Deep error analysis is covered later. As pictured below a collection of profiles was processed. Note their horizontal orientation is reversed, this is due to the reversal of the beam scan (the stage has two directions) this can easily be interchanged by simply reversing the order of voltage data.

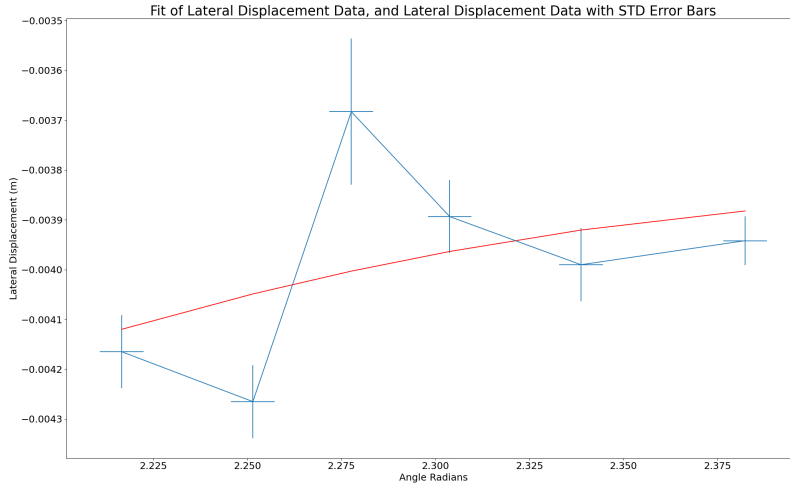


**Dataset 1 Moment Calculations Multiplot**

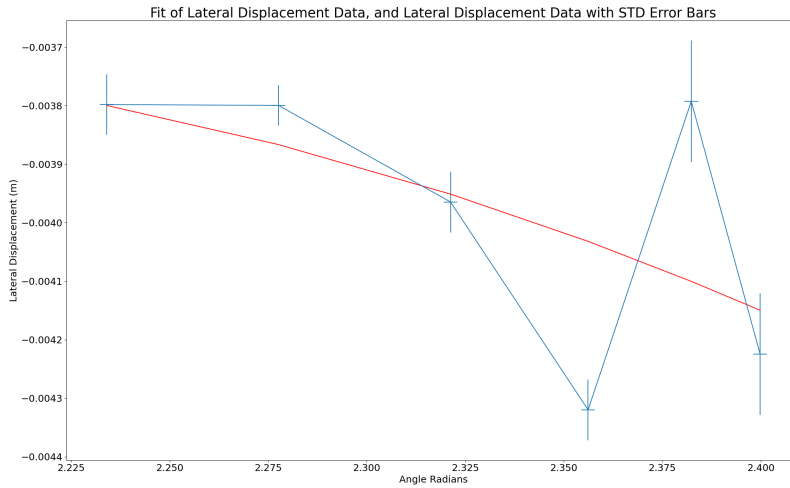


### Dataset 2 Moment Calculations Multiplot

This analysis yielded central moments for each beam profile, which allow them to be interpreted under the deflection model of Snell's law. Since data was collected for beam displacement and incident angle, the previous representation of Snell's law was re-arranged to allow for a model with parameters  $n_{glass}$  (index of refraction of the glass) and a zero angle. The zero parameter was unnecessary to find the uncertainty and index of refraction of the glass, but was useful in simplifying determining the uncertainty of the index of refraction of the glass. As another simplifying choice instead of fitting Snell's law for the lab setup in terms of displacement versus angle, a model was fit of the derivative of displacement with angle. This choice gives equivalent fitting and error analysis (besides losing a single data point of information out of order 10), but does not have an arbitrary initial value for displacement (similar to the choice of fitting the zero point instead of specifying it), due to the derivative, which would have been difficult to determine systematically. The model then could be fit to these moments using basic least squares tools available in most numerical suites. This yielded an estimated value for a true zero of the displacement, and gave an estimated value for the index of refraction of the glass. Below is a fit of the displacement derivatives with angle to the model.



### Dataset 1 Model Fit



### Dataset 2 Model Fit

**Error Analysis** By simple analysis of moments and the finite derivative we can find the uncertainty in the moments used by our full model. The full derivation is given below, intuitively we are taking the moment of a derivative, and

moments contain an integral in their denominator, thus the denominator will just depend on the voltage reading at boundaries, and the numerator will also simplify upon inspection. The central moment is  $M$ , the raw voltage readings are  $V_i$  being zero indexed,  $\sigma V$  is the standard deviation of the voltage,  $\Delta x$  is the distance the stage moves between each data point,  $D_i$  are the finite differences between  $V_i$ , and  $V_m, V_0$  are the first and last voltage readings, which with the razor profile will be maximum and minimum voltage readings.

$$M = \frac{\sum_0^{N-2} D_i(i+1)\Delta x}{\sum_0^{N-2} D_i} \quad (2)$$

$$M = \frac{\Delta x S}{V_{N-1} - V_0} \quad (3)$$

$$S = 1(V_1 - V_0) + 2(V_2 - V_1) + 3(V_3 - V_2) \dots \quad (4)$$

$$+ (N-4)(V_{N-3} - V_{N-4}) + (N-3)(V_{N-2} - V_{N-3}) + (N-2)(V_{N-1} - V_{N-2}) \quad (5)$$

$$S = (N-2)V_{N-1} - V_0 - \sum_1^{N-2} V_i \quad (6)$$

$$M = \Delta x \frac{(N-2)V_{N-1} - V_0 - \sum_1^{N-2} V_i}{V_{N-1} - V_0} \quad (7)$$

Terms are now isolated into useful groups, note the sum term will act in a Gaussian manner, since  $V_i$ 's are iid except for their mean.

$$\frac{dM}{dV_{N-1}} = \Delta x \frac{(V_{N-1} - V_0)(N-2) - ((N-2)V_{N-1} - V_0 - \sum_1^{N-2} V_i)}{(V_{N-1} - V_0)^2} \quad (8)$$

$$\frac{dM}{dV_{N-1}} = \Delta x \frac{\sum_1^{N-2} V_i - V_0(N-3)}{(V_{N-1} - V_0)^2} \quad (9)$$

$$\frac{N}{2}(V_{N-1} + V_0) \quad (10)$$

Note  $V_0$  is very small compared to the sum which is approximately equal to:

$$\frac{N}{2}(V_{N-1} + V_0) \quad (11)$$

$$\left| \frac{dM}{dV_{N-1}} \right| \cong \Delta x \frac{N(V_{N-1} + V_0)}{2(V_{N-1} - V_0)^2} \quad (12)$$

$$(13)$$



## 0.4 Results

---

The same process and approximations yield a symmetric equation for the partial with  $V_0$ , as expected since  $V_0$  appears symmetrically in the equations.

$$\left| \frac{dM}{dV_0} \right| \cong \Delta x \frac{N(V_{N-1} + V_0)}{2(V_{N-1} - V_0)^2} \quad (14)$$

We combine these two symmetric terms by rough approximation (of a small sum, two elements) by taking one and multiplying it by  $\sqrt{2}$  when determining a total uncertainty for  $M$ . The sum terms are numerous and as mentioned should be treated as a normal distribution, which has a very small variance, so we will ignore it. We get a final and useful approximation of the uncertainty in the moment as Eqn. 16. Eqn 15. is the insignificant Gaussian noise in the moment due to the bulk Voltage measurements.

$$\sigma M_{\Sigma} = \Delta x \frac{\sigma V}{\sqrt{N}(V_{N-1} - V_0)} \quad (15)$$

$$\sigma M \cong \Delta x \frac{N(V_{N-1} + V_0)}{(V_{N-1} - V_0)^2 \sqrt{2}} \sigma V \quad (16)$$

The moment error now being found, and our other parameter measured simply being degrees off of a vernier scale, which had a human error STD. of 6 minutes. Since a model fit was used to determine the parameter  $n_{glass}$ , the error had to be determined by taking finite partial derivative approximations of the parameter  $n_{glass}$  and then using normal Pythagorean error propagation. These finite derivatives were taken programmatically. In practice the precision of the angular measurements were sufficient that when accounting for the derivative of parameters the impact of angular deviations were not significant for error determination but were calculated regardless.

**Semi Circular Block** A semi circular block was placed aligned to the perpendicular of the laser setup. The block was chosen to be semi circular to ensure that the beam could only be reflected upon exiting the medium regardless of its angle, so that the critical angle could be determined. The critical angle was determined by finding a zero angle, where the beam was not deflected at all, and then finely adjusting the rotation of the circular block until the intensity of the transmitted light dropped sharply and was not visible to the human eye. This yielded somewhat acceptable results, although error bars were at minimum of order 10% due to low accuracy of the zero angle, and failing to take symmetric data (Negative angles of the rotation stage).

## 0.4 Results

### Profiling Method for Glass Plate

Of two runs of the experiment:

## 0.5 Data Tables

---

Dataset 1 gave:  $n_{glass} = 1.51$ ,  $\sigma n_{glass} = 0.01$   $\theta_0 = 140$  deg  $\sigma\theta_0 = 2$  deg  
Dataset 2 gave:  $n_{glass} = 1.48$ ,  $\sigma n_{glass} = 0.02$   $\theta_0 = 119$  deg  $\sigma\theta_0 = 3$  deg  
Together:  $n_{glass} = 1.500$ ,  $\sigma n_{glass} = 0.012$

### Critical Angle Method for Acrylic Block $n_{block} = 1.4$ $\sigma n_{block} = 0.2$

This was calculated using the critical angle equation  $\theta_{critical} = \text{asin}(\frac{n_{air}}{n_{?}})$  with  $\theta_{critical} = 45.3$ , achieving error bars by allowing the measured angle from zero to deviate a full degree both ways. Clearly the zeroing method we chose is not better than order 1 degrees, since the measured zero for the profiling method was order 1 degrees off of the model fit in both cases, with the model fit having order 1 degrees uncertainty as well.

## 0.5 Data Tables

Python and Matlab files generate and or load this data. Full profiles are contained in the mat files labeled with degree values, mirrored is the second dataset. See the output\_python.txt in the matlab folder for moments etc.

```
ANG D1 [2.19911486 2.23402144 2.26892803 2.28638132 2.32128791 2.35619449
2.40855437]
mom_D1 [0.002705 0.00255962 0.00241074 0.00234646 0.00221054 0.00207125
0.00186485]
ANG D2 [2.21656815 2.25147474 2.30383461 2.3387412 2.37364778 2.39110108
2.40855437]
mom_D2 [0.00248443 0.00235186 0.00215292 0.00201452 0.00186373 0.00179754
0.00172381]
DOMAIN MOM DERIV D1 [2.21656815 2.25147474 2.27765467 2.30383461 2.3387412 2.38237443]
DOMAIN MOM DERIV D2 [2.23402144 2.27765467 2.32128791 2.35619449 2.38237443 2.39982772]
MOM DERIV D1 [-0.00416483 -0.00426509 -0.00368302 -0.00389373 -0.00399025 -0.00394204]
MOM DERIV D2 [-0.00379804 -0.00379953 -0.00396461 -0.00431993 -0.00379243 -0.00422446]
MOMENT UNCERTAINTIES D1 [5.19294018e-05 5.19294018e-05 1.03858804e-04 5.19294018e-05
5.19294018e-05 3.46196012e-05]
CORRECT_N2_SIGMA_TOTAL_NM, ZERO_NM_SIGMA: 0.011289789537682568 0.038855500382811
DERIV FIT NONMIRROR
[5.19294018e-05 5.19294018e-05 1.03858804e-04 5.19294018e-05
5.19294018e-05 3.46196012e-05]
n GLASS: 1.5149718115965425 zero: 2.459587133384254
```

```
MOMENT UNCERTAINTIES D2 [5.19294018e-05 3.46196012e-05 5.19294018e-05 5.19294018e-05
1.03858804e-04 1.03858804e-04]
CORRECT_N2_SIGMA_TOTAL_MIRR, ZERO_NM_SIGMA: 0.021188986020122785 0.05544035714958311
DERIV FIT MIRROR
```

## 0.5 Data Tables

---

```
[5.19294018e-05 3.46196012e-05 5.19294018e-05 5.19294018e-05  
1.03858804e-04 1.03858804e-04]  
n GLASS: 1.4841567245176068 zero: 2.0845362949044244
```